OFFICE OF NAVAL RESEARCH

Contract No. N00014-91-J-1409

Technical Report No. 122

Observing Chemical Transformations by Atomic-Resolution Scanning Tunneling Microscopy: Sulfide Electroxidation on Au(111)

by

X. Gao, Y. Zhang, and M.J. Weaver

Prepared for Publication

in the

Journal of Physical Chemistry

Purdue University

Department of Chemistry

West Lafayette, Indiana 47907

May 1992

ABSTRACT

The prospects of utilizing atomic-resolution scanning tunneling microscopy (STM) as a real-space in-situ probe of molecular transformations on electrochemical surfaces are illustrated for the specific case of sulfide electrooxidation on Au(111) in aqueous solution. At relatively low electrode potentials, sulfide adsorption yields ordered ($\sqrt{3} \times \sqrt{3}$)R30° layers. The onset of sulfide electrooxidation produces marked changes in the adsorbate structure, arrays of rectangular close-packed structures being formed which consist predominantly of S_8 rings. The ring dimensions, including the S-S bond distances, differ significantly from bulk-phase polysulfur, being affected apparently by the gold substrate structure. Further reaction yields multilayer S_x structures exhibiting greater disorder. The likely scope of reactive surface electrochemistry amenable to STM is noted.

The increasing emergence of scanning tunneling microscopy (STM) as a means of obtaining atomic-level structural information at metal surfaces is promising to foster a new era in surface science.[1] The technique has recently been demonstrated to yield *true* atomic resolution (i.e., identification of individual surface atoms) at in-situ electrochemical (metal-solution) interfaces as well as on metal surfaces in ultrahigh vacuum (uhv).[2-5] Besides the practical as well as fundamental importance of the former systems, they offer an intriguing opportunity to examine the effect of varying the electronic surface charge, and hence the electrode potential, on the surface atomic structure. So far, electrode potenti -dependent adsorbate structures on ordered transition metals[2-4] and reconstruction of low-index gold surfaces[5-7] have been reported along these lines.

A central tactic in electrochemistry is the utilization of controlled alterations in electrode potential to trigger surface redox transformations. Such processes range from outer-sphere electron transfer, where the reactant-surface interactions are usually weak and nonspecific, to a diverse array of multi-electron reactions involving chemisorbed species. In-situ spectroscopic, especially molecular vibrational, techniques are contributing importantly to the identification and characterization of such reactive electrochemical adsorbates.[8,9] The advent of complementary information on the real-space structures for molecular adlayers involved in (or formed by) such processes, as might be provided by in-situ STM, would clearly be of great value and significance.

We present here the first STM results of this type, specifically for the electrooxidation of sulfide on ordered Au(111) in aqueous media. This system was selected partly in view of the extensive information available for sulfur adlayers in metal-gas systems, including recent STM data,[1,10,11] and because of the availability of recent in-situ surface-enhanced Raman spectroscopic

information on the electrooxidation process.[12] The latter indicates the transformation of monomeric adsorbed sulfur into polymeric species, probably S_8 rings, triggered by sulfide electrooxidation in both acidic and alkaline aqueous media.[12] The present STM results also indicate the potential-dependent occurrence of such a surface molecular transformation; however, the ordered close-packed adlayer thus formed consists of cyclical structures that differ significantly from bulk-phase S_8.

The experimental STM procedures are largely as described elsewhere.[3-5,13] The microscope is a commercial Nanoscope II (Digital Instruments) with a bipotentiostat for electrochemical STM. The STM tips were 0.01 in. tungsten wire etched electrochemically in 1 M KOH, and insulated with clear nail polish (Wet 'n Wild, Pavion, Ltd.) so to minimize the occurrence of faradaic electrochemistry on the wire. Most STM images were obtained in the so-called "height mode" (i.e., at constant current). The set-point current was typically 10-20 nA, and the bias voltage 10-50 mV. (The images were essentially unaffected by the sign of the latter.) The Au(111) crystal (hemisphere, 7 mm diameter)[14] was flame annealed, cooled in ultrapure water, and transferred to the STM cell protected by a drop of water. The $Na_2S \cdot 9H_2O$ (Aldrich) was purified as in ref. 12. A Pt wire was used as a quasi-reference electrode in the STM cell, but all potentials are quoted below versus the saturated calomel electrode (SCE).

Figures 1A-E show a representative set of STM images, obtained mostly under electrode-potential control in aqueous 0.1 M $NaClO_4$ + 4 mM $HClO_4$ containing 0.5 - 1 mM Na_2S. At the most negative potentials, -0.5 V vs SCE, that can be attained on Au(111) in this media (due to the onset of hydrogen evolution), atomic-resolution images of the Au(111) substrate were obtained, essentially identical to those reported in ref. 6. These consisted of hexagonal spots (corresponding to Au surface atoms), spaced 2.9Å apart. (The Au interatomic

spacing provided a convenient calibration check of the x-y piezoelectric drivers.) At less negative potentials, ca -0.4 to -0.1 V, images showing large (at least 200 x 200Å) domains having a different symmetry were obtained, an example of which is shown (in unfiltered large-scale form) in Fig. 1A.

This structure can readily be deduced to have the symmetry ($\sqrt{3}$ x $\sqrt{3}$)R30° with respect to the gold substrate lattice. Thus the rows of bright spots (i.e., large z-displacement) lie in directions midway between (i.e., 30° rotated from) those for the gold substrate images. Also, the spacing between the spots, 5.0 ± 0.2Å, matches well that expected for a ($\sqrt{3}$ x $\sqrt{3}$) adlattice on gold (i.e., $\sqrt{3}$ x 2.9Å). This structure can confidently be deduced to consist of adsorbed monomeric sulfur with fractional coverage 1/3. The same unit cell has been deduced commonly for sulfur adlayers on several face-centered cubic transition-metal (111) surfaces in uhv by low-energy electron diffraction (LEED).[15] A ($\sqrt{3}$ x $\sqrt{3}$)R30° structure has also been observed recently for STM for alkylthiol films, involving monomeric sulfur surface binding, on Au(111) in air.[11] The surface Raman spectra on polycrystalline gold at these electrode potentials show only a single vibrational band at 300 cm^{-1}, consistent with a metal-adsorbate stretch involving sulfur atoms.[12] Some STM data contained adjoining patches where the substrate lattice and the sulfur adlattice were obtained. These combined images suggest that the sulfur binding site is a threefold hollow, in accordance with LEED analyses for the metal-uhv systems.[15] The relatively small z-corrugation, ca 0.6Å, observed in the ($\sqrt{3}$ x $\sqrt{3}$) images also supports this assignment. Shifting the potential negative to ca -0.5 V yielded a reversible removal of the ($\sqrt{3}$ x $\sqrt{3}$) structure, suggesting the occurrence of sulfide desorption, in accord with the surface Raman data.[12] (Ordered rows of sulfur atoms, however, remained on the terrace edges under these conditions, indicating stronger adsorbate binding at these sites.)

Altering the potential to more positive values, above ca -0.1 V, yielded dramatic alterations in the STM images. These conditions correspond to the onset of detectable faradaic currents, involving the net anodic formation of polysulfides from solution H_2S.[12] After 1-2 min., rectangular- or square-like ring structures become discernable. In many instances, long-range superstructures formed by rectangular-packed arrays are formed. Figures 1B and C show a pair of representative height-shaded images (displayed 30° from the surface normal) obtained in this manner. The former contains three distinct elements. Recognizable in the far top-right hand corner and in the lower portion of Fig. 1B are surviving patches having ($\sqrt{3} \times \sqrt{3}$) symmetry, i.e., of monomeric sulfur. In the lower left-hand region are seen loosely packed and somewhat disordered rings. The upper region of Fig. 1B, however, is dominated by an ordered rectangular array of such rings. A magnified portion of a related, yet distinct, array of rings is shown in Fig. 1C, which was mildly filtered by Twodfft process. Evident upon close inspection are left- and right-hand edges consisting of linear trios of spots; these edges are separated by 4.8 ± 0.3Å, the trio members being 2.6 ± 0.2Å apart. Interestingly, the long axis of the unit cell in Fig. 1C parallels closely the underlying rows of gold atoms. This correspondence between the overlayer and metal substrate directions was usually, but not always, observed; the adlayer row directions in Fig. 1B deviate by about 15° from the substrate rows.

Although several subtly different ring structures were obtained, in some cases it is possible to discern eight individual spots (and hence presumably sulfur atoms) in a given ring. An example is displayed in magnified form in Fig. 1D (filtered in the same way as 1C); this image of crown-like structures was obtained on Au(111) in air after transfer from the solution environment. Similar images of cyclic sulfur structures on Au(111) in air have recently been obtained

by Porter et al.[16] Some images containing rectangular symmetries as in Figs. 1B and C also exhibited a weaker spot along the rectangle joining the triplet pairs; we therefore have reason to believe that these various ring species contain eight sulfur atoms. Returning the potential to more negative values, ca −0.4 V, resulted in the removal within 1–2 min. of the polysulfur species and the reappearance of the monomeric ($\sqrt{3} \times \sqrt{3}$) sulfur adlayer. This transition is consistent with both the surface Raman and electrochemical data, which indicate that polysulfur electroreduction to sulfide occurs under these conditions.[12]

Having deduced the presence of arrays of S_8–like surface species formed by sulfide electrooxidation, at first sight it appears that conventional sulfur catenation chemistry is occurring. Nevertheless, an intriguing as well as unexpected feature of these structures concerns the inferred S–S bond distances, d_{s-s}. Values of d_{s-s} in polysulfur (and polysulfide) span a narrow range, 2.0 – 2.1Å.[17] As already mentioned, however, in most cases where individual sulfur atoms (or groups of atoms) can be resolved in the STM images, longer interatomic distances, in the range 2.3–2.7Å, are obtained. While the evaluation of such distances by STM is subject to some uncertainty, they are reproducible to within ±5–10%; the piezoelectric calibration could readily be checked in a given experiment from the Au(111) substrate or ($\sqrt{3} \times \sqrt{3}$) sulfur adlayer images.

Ordered arrays of sulfur ring–like structures, containing 3,4, or 6 atoms, have been observed by STM to form at higher sulfur coverages on the hexagonal–symmetry Re(0001) surface in uhv.[1,10] Although the formation of such rings indicates the presence of some S–S bonding, the d_{s-s} values are also abnormally large, 2.75Å. Such a spacing, equal to the Re–Re distance, enables the ordered sulfur adlayer to be commensurate with the metal lattice with the S atoms located in threefold hollow sites.[1,10]

It seems reasonable to assert that related crystallographic factors play a role in the present system. Intriguingly, the rectangular "S_8" structures such as those in Fig. 1C have a size and shape that is nearly commensurate with the underlying gold lattice. Thus the distance between the sulfur trio members lying along the Au rows, 2.6Å, is not much shorter than the Au–Au separation, 2.88Å, and the length across the rectangle, 4.8Å, approximates the separation ($\sqrt{3}$ x 2.88Å) between adjacent parallel Au rows. The tendency of the ordered polysulfur arrays to propagate along Au atomic rows further supports this notion. One can envisage, then, the S–S bond lengths to be elongated from 2.1Å and the bond angles modified so to both bind to, and pack two-dimensionally on, the ordered metal surface. Aside from the Re–S system noted above, there is precedent from bulk-phase sulfur chemistry that S–S bonds as long as 3Å can form in compounds containing other elements.[18] A related, yet distinct, possibility is that cyclic gold polysulfide complexes are being formed on the surface. A variety of such sulfur compounds, including gold complexes,[19] are known in which one or more metal atoms are incorporated into the ring.[20]

Additional polysulfur layers are formed with increasing time, especially if the sulfur deposition rate is enhanced by increasing the electrode potential. These layers usually appear less ordered, although sulfur ring structures still predominate (as in Fig. 1B). Figure 1E is an example of large-scale STM images obtained for multilayer sulfur films under these conditions. Several types of larger ring structures were observed, for example, a S_{12} ring is seen in the center of 1E. Unlike the ordered sulfur adlayers, however, molecular resolution is not easily achieved and the images are usually unstable. These properties presumably reflect the difficulties associated with longer-range electron tunneling and of imaging more mobile molecules. The extraction of reliable d_{s-s} values from such STM data is largely precluded, although images were occasionally

obtained with sufficient resolution to indicate S_8 and S_{10} rings with shorter (ca 2.0–2.2Å) d_{s-s} values. Preliminary STM data obtained for sulfide electrooxidation on ordered Au(110), however, signal the presence of relatively disordered S_8 layers with conventional (2.1Å) S–S bond distances and ring conformations.

Even though the sulfide/sulfur redox system displays some complexities, the foregoing demonstrates the degree of atomic-level structural information for electrochemical molecular transformations that can be extracted readily by means of in-situ STM. Careful insulation of the tip material can enable atomic-resolution images to be obtained even during the occurrence of significant faradaic (i.e., redox) electrochemistry at the substrate surface; thus in this case, much higher, *ca* 10 μA, *faradaic currents can flow (between the working and* counter electrodes) than those, < 20 nA, resulting from electron tunneling to and from the STM tip. The scope of atomic-level STM applications of this type should be broad indeed, encompassing examinations of the metal lattice structure as well as molecular adsorbate transformations during electrocatalytic (and possibly corrosion) processes.

ACKNOWLEDGMENTS

We are grateful to Dr. Antoinette Hamelin for preparing the ordered Au(111) surface. We thankfully acknowledge support of this work by the Office of Naval Research and the National Science Foundation.

REFERENCES AND NOTES

1. For an insightful recent review, see: Ogletree, F.; Salmeron, M., Prog. Solid State Chem., 1990, 20, 235

2. Magnussen, O.M.; Hotlos, J.; Nichols, R.J.; Kolb, D.M.; Behm, R.J., Phys. Rev. Lett., 1990, 64, 2929

3. S.-L. Yau; C.M. Vitus; B.C. Schardt, J. Am. Chem. Soc., 1990, 112, 3677

4. Yau, S.-L.; Gao, X.; Chang, S.-C.; Schardt, B.C.; Weaver, M.J., J. Am. Chem. Soc., 1991, 113, 6049

5. Gao, X.; Hamelin, A.; Weaver, M.J., Phys. Rev. Lett., 1991, 67, 618

6. (a) Gao, X.; Hamelin, A.; Weaver, M.J., J. Chem. Phys., 1991, 95, 6993; (b) Tao, N.J.; Lindsay, S.M., Applied Physics, 1991, 70, 5141

7. Gao, X.; Hamelin, A.; Weaver, M.J., Phys. Rev. B, 1991, 44, 10983

8. For reviews, see: Compton, R.G. and Hamnett, A. (editors), "Comprehensive Chemical Kinetics", Vol. 29, Elsevier, Amsterdam, 1989

9. For example: Weaver, M.J.; Corrigan, D.S.; Gao, P.; Gosztola, D.; Leung, L.-W.H., J. Electron. Spect. Related Phenom., 1987, 45, 291; ACS Symp. Ser., 1988, 378, 303

10. (a) Ogletree, D.F., et al., J. Vac. Sci. Tech., 1990, A8, 297; (b) Ogletree, D.F., et al., J. Vac. Sci. Tech., 1991, B9, 886; (c) Hwang, R.Q., et al., Phys. Rev. B, 1991, 44, 1914

11. Widrig, C.A.; Alves, C.A.; Porter, M.D., J. Am. Chem. Soc., 1991, 113, 2805

12. Gao, X.; Zhang, Y.; Weaver, M.J., Langmuir, 1992, 8, 668

13. Vitus, C.; Chang, S.-C.; Schardt, B.C.; Weaver, M.J., J. Phys. Chem., 1991, 95, 7559

14. The Au(111) crystal (nominal orientation ±0.25°) was grown, cut, and polished in Laboratorie d'Electrochimie Interfaciale du C.N.R.S., Meudon, France, by Dr. A. Hamelin.

15. (a) Chan, C.-M.; Weinberg, W.H., J. Chem. Phys., 1979, 71, 3988; (b) Hayek, K., et al., Surface Science, 1985, 152, 419; (c) Maca, F.; Scheffler, M.; Berndt, W., Surface Science, 1985, 160, 467; (d) Koestner,

R.J.; Salmeron, M.; Kollin, E.B.; Gland, J.L., Surface Science, 1986, 172, 668; (e) Wong, P.C.; Zhou, M.Y.; Hui, K.C.; Mitchell, K.A., Surface Science, 1985, 163, 172

16. Widrig, C.A.; Alves, C.A.; Porter, M.D., in preparation.

17. For a review, see: Meyer, B., Chem. Revs., 1976, 76, 367

18. Steudel, R., Angew. Chem. Int. Ed. Eng., 1975, 14, 655

19. (a) Clark, G.R.; Russell, D.R.; Roper, W.R.; Walker, A., J. Organomet. Chem., 1977, 136, C1; (b) Marbach, G.; Strähle, J., Angew. Chem. Int. Ed. Eng., 1984, 23, 246; (c) Fackler, J.P.; Porter, L.C., J. Am. Chem. Soc., 1986, 108, 2750

20. Müller, A.; Diemann, E., Adv. Inorg. Chem., 1987, 31, 89

FIGURE CAPTIONS

Fig. 1

STM images of Au(111) surface in aqueous 0.1 M $HClO_4$ + 4 mM $HClO_4$ + 0.5 mM Na_2S, showing surface molecular transformation induced by sulfide electrooxidation. A). Unfiltered large scale topview image of ($\sqrt{3}$ x $\sqrt{3}$)R30° domain. Electrode potential E = -0.3 V vs SCE. B). Height-shaded image, after holding at E = 0 V for 30 min. C). Close-up image of domain prepared similarly to B. D). Example of sulfur adlayer domain observed after transfer to air. E). Example of multilayer containing different sulfur cyclical structures. Tunneling conditions: bias voltage = 20-50 mV, tunneling current = 10-20 nA, in constant current mode ("height mode"). Figures 1C and 1D were mildly filtered by 2dfft process to remove high-frequency noise; 1E was low-pass filtered.

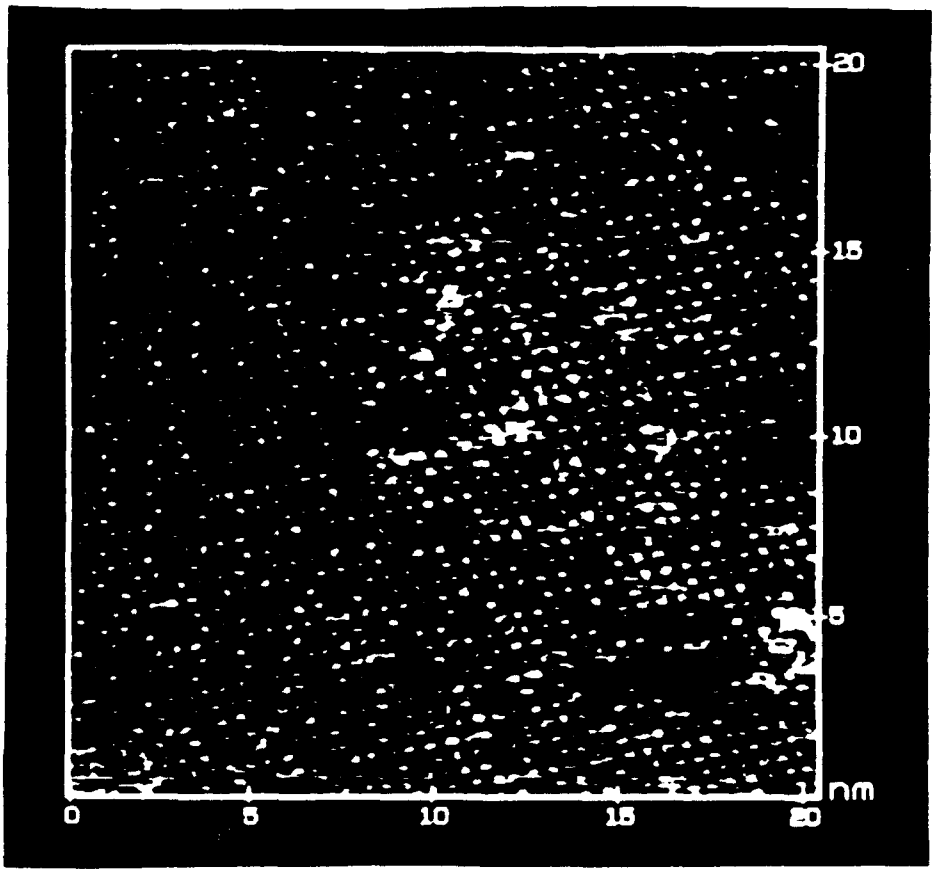

FIG 1A

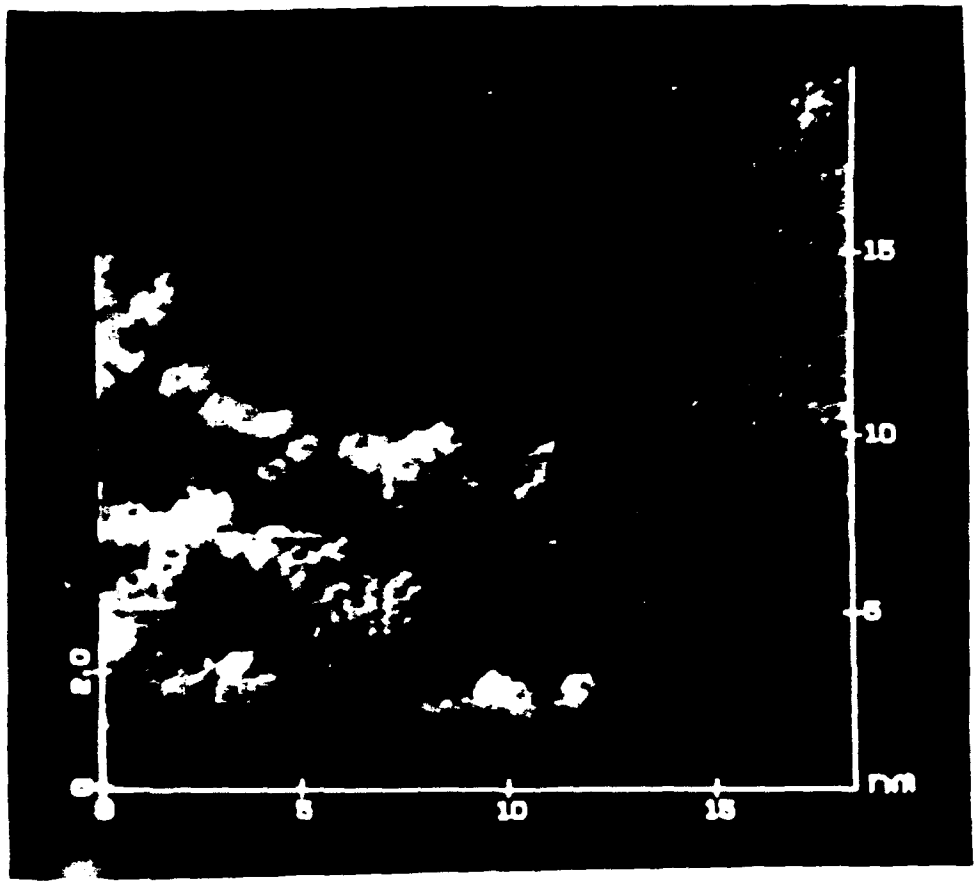

FIG 1B

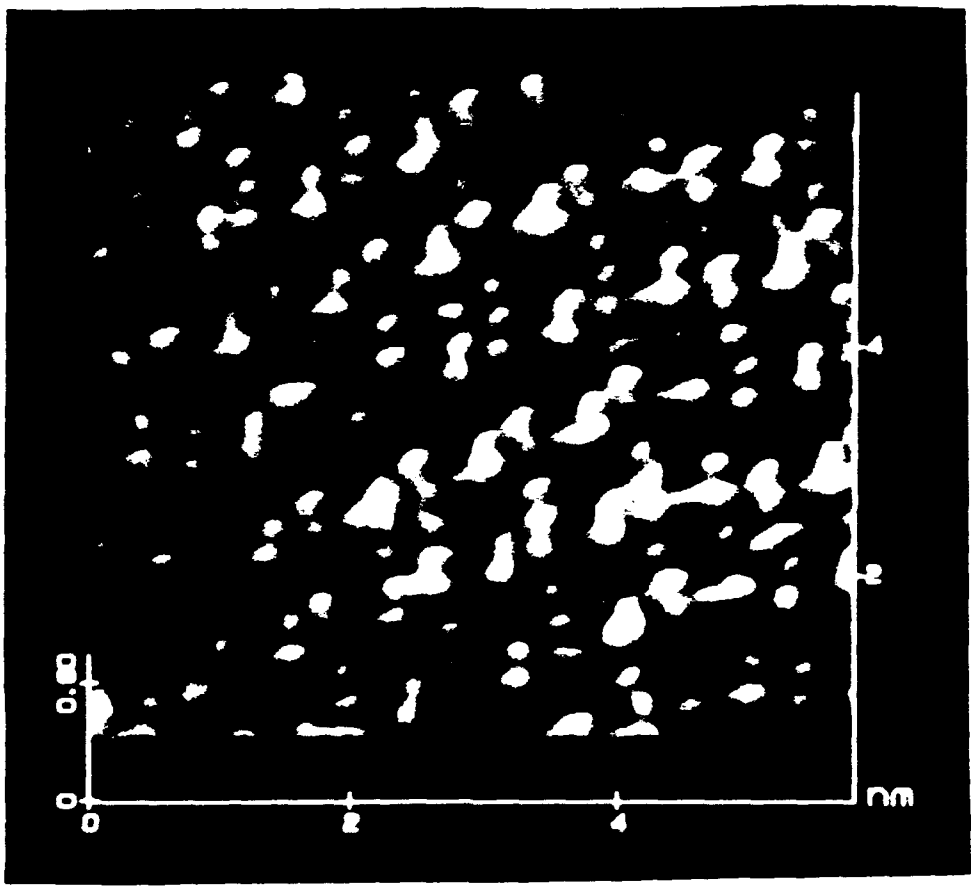

FIG 1C

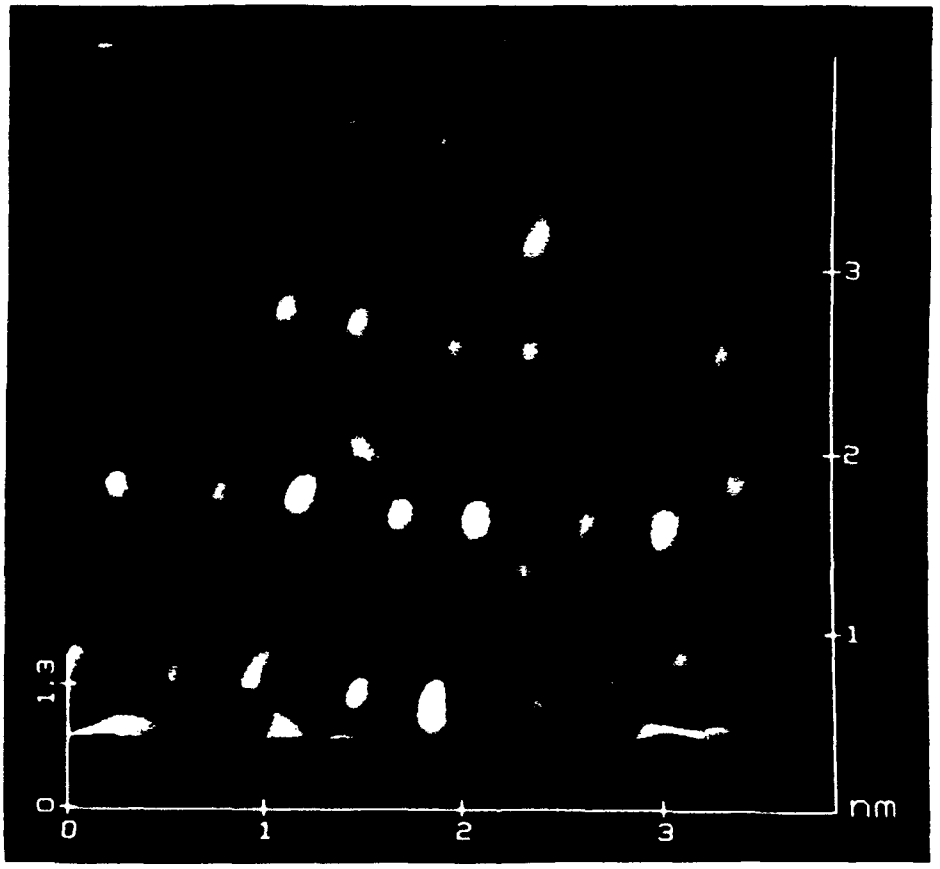

FIG 1D

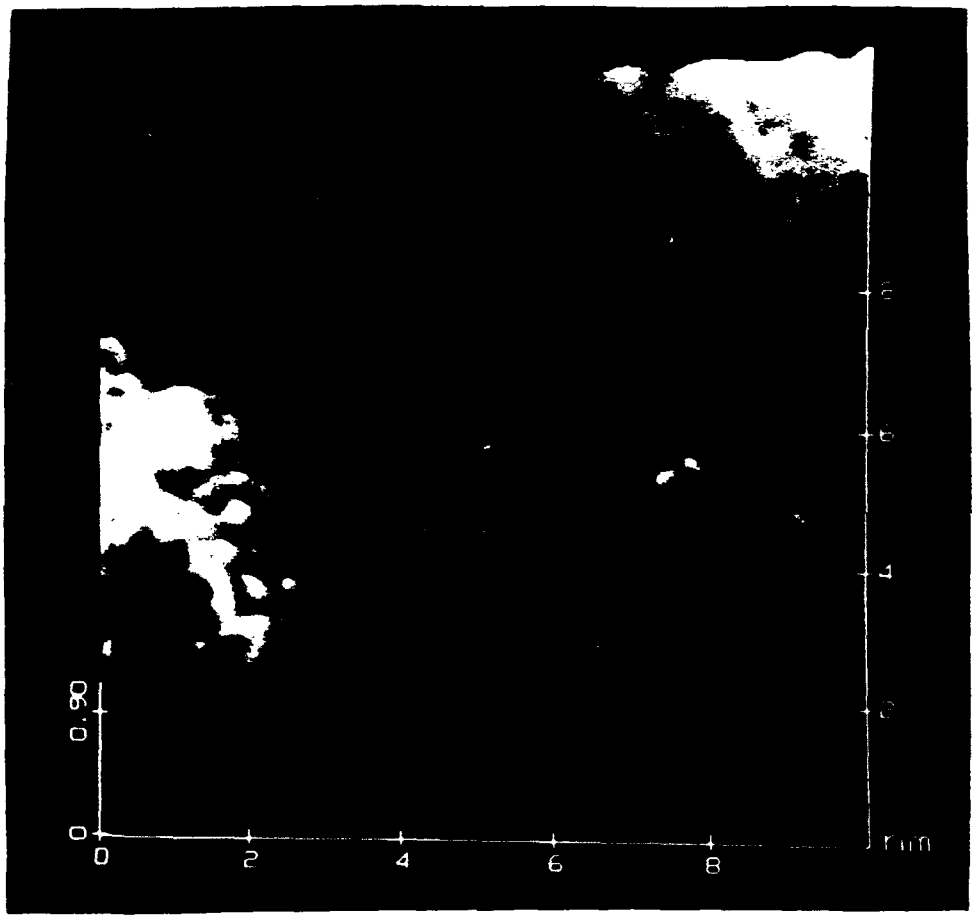

FIG 1E